Random Telegraph Noise in Highly Scaled nMOSFETs

J.P. Campbell[1], J. Qin[1,2], K.P. Cheung[1*], L.C. Yu[1,3], J.S. Suehle[1], A. Oates[4], K. Sheng[3]
[1]Semiconductor Electronics Division, NIST, Gaithersburg, MD 20899 *kpckpc@ieee.org
[2]Department of Mechanical Engineering, University of Maryland, College Park, MD 20740
[3]Department of Electrical and Computer Engineering, Rutgers University, Piscataway, NJ 08854
[4]TSMC Ltd., Hsin-Chu, Taiwan 300-77, R.O.C.

Abstract— **Recently, 1/f and random telegraph noise (RTN) studies have been used to infer information about bulk dielectric defects' spatial and energetic distributions. These analyses rely on a noise framework which involves charge exchange between the inversion layer and the bulk dielectric defects via elastic tunneling. In this study, we extracted the characteristic capture and emission time constants from RTN in highly scaled nMOSFETs and showed that they are inconsistent with the elastic tunneling picture dictated by the physical thickness of the gate dielectric (1.4 nm). Consequently, our results suggest that an alternative model is required and that a large body of the recent RTN and 1/f noise defect profiling literature very likely needs to be re-interpreted.**

Keywords-Random Telegraph Noise, 1/f noise, elastic tunneling

I. INTRODUCTION

Noise in device drain currents (I_D) has been used for many decades as an indicator of device performance and reliability [1-3]. Recently, noise has been subject to a renaissance as the geometry of many nano-scale devices precludes "conventional" electrical characterization evaluations (capacitance and charge pumping measurements). Whereas scaling makes these conventional electrical measurements more difficult, it actually makes the observance of many noise phenomena easier [4, 5]. This unique scaling property has led to noise imposed performance and reliability limits in SRAM and FLASH memory technologies [6-9]. It has also led many researchers to employ noise characterizations to infer details about dielectric defects in advanced gate stacks [10-12] and most recently to probe the fundamental mechanisms behind the elusive negative bias temperature instability (NBTI) [13].

Unfortunately, these clever noise characterizations all rely on models of noise which are far from unified. Many researchers base their analysis on the seminal work of McWhorter [3]. In this noise paradigm, the measured device drain current (I_D) noise is due to *elastic* tunneling of inversion layer charge carriers to and from dielectric defects (Fig. 1a). In this model each elastic tunneling event is associated with a characteristic time constant related to the dielectric defect's depth profile. Each of these discrete tunneling events is observable as a "digital" I_D fluctuation in the time domain and as a Lorentzian spectrum (slope = $1/f^2$) in the frequency domain (Fig. 1b). These digital fluctuations are often referred to as random telegraph noise (RTN) [14]. The summation of all RTN events, each with different characteristic time constants, is surmised to be the origin of the universally observed 1/f noise characteristic in the frequency domain (Fig. 1c) [2]. Since this model links the observed noise characteristics to dielectric defects, many researchers have extended the McWhorter model to interpret 1/f and RTN measurements as indicators of dielectric defects' energetic and spatial distributions (defect profiling) [10-12, 15-21]. Quite recently, 1/f noise profiling has been used in combination with frequency-dependent charge-pumping to suggest that electrical stress generates defects in high-k dielectric layers of advanced gate stacks [11]. Such work has sparked a controversy with far-reaching implications on the reliability of advanced high-k/metal gate technology.

Despite the very wide utilization of the elastic tunneling model, it is not universally accepted. On the basis of temperature activation of the observed noise spectrum, other researchers have invoked a noise model in which 1/f and RTN are dominated by *inelastic* tunneling of inversion layer charge carriers to and from dielectric defects [22, 23]. Still, others have argued on the basis of a correlation between 1/f noise and charge pumping measurements that 1/f and RTN are dominated by interface state capture and emission of inversion layer charge [24, 25]. Despite experimental evidence, neither of these alternative explanations was strong enough to supplant the general acceptance of the *elastic* tunneling noise framework. As the scaling-induced limitation on conventional electrical characterization will likely entice more researchers to employ noise measurements, it is imperative that the fundamental origins of 1/f and RTN (elastic/inelastic/interface states) be resolved.

In this paper, we present RTN measurements on highly scaled devices (physical dielectric thickness of 1.4 nm) from the sub-threshold to super-threshold regimes which clearly rule out the prevailing elastic tunneling noise model. These measurements reveal very large RTN fluctuations which enable highly reliable characteristic time constant extraction. The extracted capture and emission time constants are orders of magnitude larger than expected from the tunneling time restriction set by the dielectric thickness. This disagreement clearly rules out the widely accepted McWhorter noise model. Furthermore, our results call into question much of the RTN and 1/f noise defect profiling analysis in the recent literature.

U.S. Government work not protected by U.S. copyright

Authorized licensed use limited to: NIST Research Library. Downloaded on September 30, 2009 at 15:40 from IEEE Xplore. Restrictions apply.

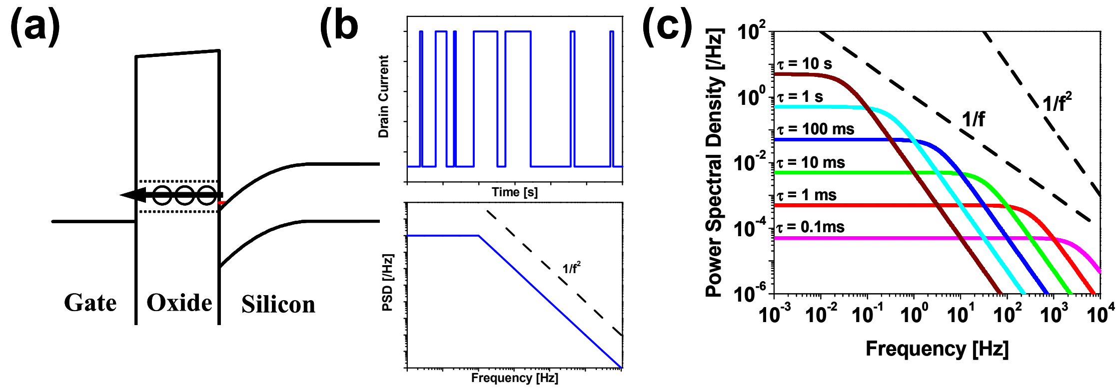

Figure 1. Schematic representation of the McWhorter model for noise. In this model, 1/f noise is assumed to originate from elastic tunneling of inversion layer charge carriers to bulk dielectric defects spatially distributed into the dielectric (a). Each of these elastic tunneling events contributes random telegraph noise which is recognized as a "digital" I_D fluctuation in the time domain and a Lorentzian spectrum ($1/f^2$) in the frequency domain (b). The summation of all the RTN noise arising from a distribution of defect depths and time constants results in a 1/f noise spectrum in the frequency domain (c).

II. Experimental Methods

Our experiments utilize silicon oxynitride (SiON) n-channel MOSFET devices with a physical dielectric thickness of 1.4 nm and nominal widths and lengths of 0.085 μm x 0.055 μm, respectively. The RTN measurement apparatus is schematically illustrated in Fig. 2. Source and gate electrodes are biased using battery-powered variable voltage sources, while the substrate electrode is grounded for all measurements. The drain current is monitored by a low-noise current amplifier with 30 kHz bandwidth. We have previously shown that this bandwidth is sufficient for our experiment [26]. The amplifier output is directly captured using a digital storage oscilloscope with a large memory depth (10^7 samples). These time series data are then analyzed offline to extract both the normalized power spectral density (PSD) and the characteristic RTN capture and emission time constants. A common limitation for RTN measurements is the conflicting need to measure relatively fast switching events of various durations with sufficient statistics to ensure accurate analysis. With our experimental set-up, we are able to measure a relatively large bandwidth while maintaining adequate statistics for the slower switching events. All measurements were performed at room temperature with the source electrode fixed at -50 mV.

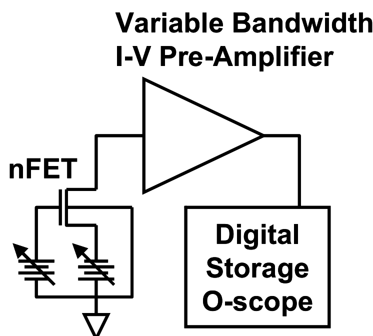

Figure 2. Schematic diagram of the experimental set-up used in this study.

Fig. 3(a) illustrates representative RTN $\Delta I_D/I_D$ fluctuations as a function of time for the sub-threshold case. The observed $\Delta I_D/I_D$ is quite large and represents a convenient "test case" in which we can unambiguously separate the high and low current states. The most commonly used parameter to describe RTN behavior is the characteristic time spent in each of the current states [14, 27]. With reference to Fig. 3(a), the low-current state occurs when an electron has been captured by a defect (which restricts current), and the high-current state occurs when the electron has been emitted (no current restriction). Consequently, the characteristic time spent in the high-current state corresponds to the capture time ($\tau_{capture}$), and the characteristic time spent in the low-current state corresponds to the emission time ($\tau_{emission}$). We extract both $\tau_{capture}$ and $\tau_{emission}$ from each RTN time series measurement by fitting the high- and low-current time distributions to an exponential of the form A*exp[-t/τ] [2]. The $\tau_{capture}$ distribution corresponding to Fig. 3(a) is shown in Fig. 3(b). The exponential fit is quite good and is representative of all our time constant extractions.

III. Results

Fig. 4 illustrates the normalized PSD as a function of gate overdrive (V_G-V_{TH}). In the sub-threshold regime, we observe very large distinct RTN fluctuations with the expected Lorentzian line shapes (slopes very close to $1/f^2$). These large RTN fluctuations (as large as 75 % $\Delta I_D/I_D$) totally dominate the device drain current. We note that increasing the gate overdrive into the super-threshold regime substantially reduces the magnitude of the RTN. Interestingly, we also note that at gate overdrives ≥ 50 mV there is a hint of a second Lorentizian line shape at lower frequencies (≈10 Hz). We postulate that this second Lorentzian line indicates the participation of a second defect which becomes more prominent at these super-threshold gate overdrives. This second defect is presumably located at a less critical location and thus has less impact on the I_D RTN. It is important to note that we are unable to determine if the second defect is gate-

Authorized licensed use limited to: NIST Research Library. Downloaded on September 30, 2009 at 15:40 from IEEE Xplore. Restrictions apply.

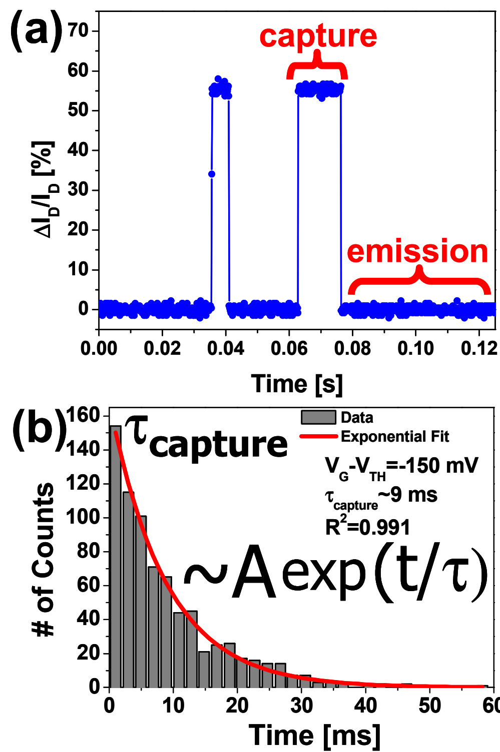

Figure 3. Representative RTN drain current (I_D) fluctuations as a function of time (a) for -150 mV gate overdrive. Note the very large percentage fluctuation. The corresponding representative distribution of time spent in the high state is illustrated in (b). The characteristic capture time constant is extracted by fitting the time distribution to an exponential. This plot (b) is representative of the good fits we obtained for our measurements.

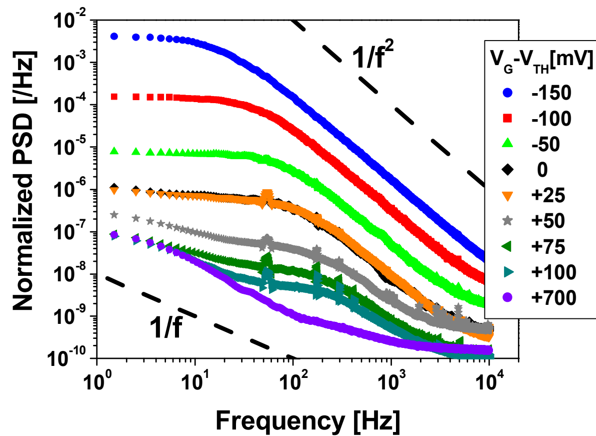

Figure 4. Normalized power spectral density as a function of gate overdrive. At lower gate overdrives, the large RTN results in a distinct Lorentzian PSD signature with slope $1/f^2$. At higher gate overdrives, we note the emergence of a second RTN fluctuation at lower frequencies. V_{TH} = 300 mV for this device.

voltage activated or if the first defect is simply less dominant at higher gate overdrives. Fig. 5 illustrates the corresponding time series traces at low-gate overdrive (Fig. 5a), moderate-gate overdrive (Fig. 5b), and at operation conditions (Fig. 5c).

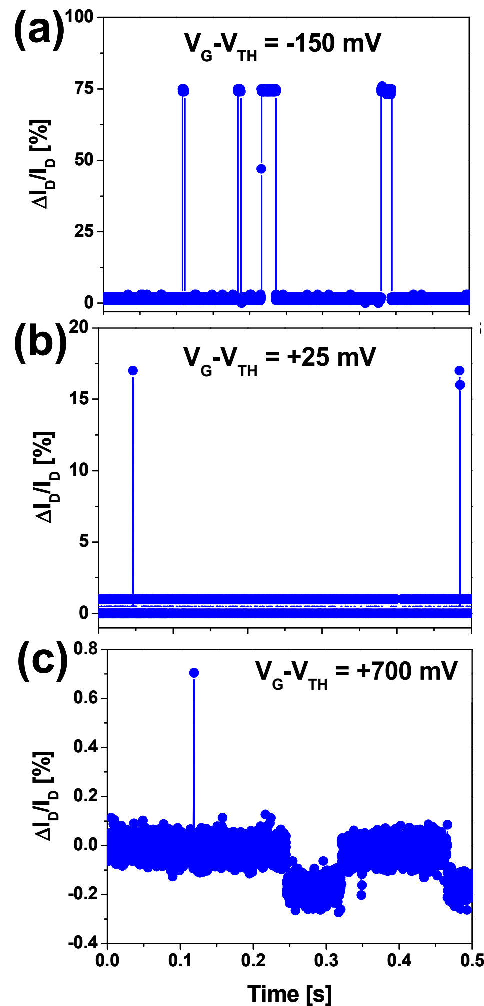

Figure 5. Drain current time series illustrating that the largest RTN (defect #1) is observed sub-threshold (a) and diminishes as the gate overdrive increases (b). At the highest gate overdrive (c), we note the presence of an additional low-frequency RTN fluctuation (defect #2). V_{TH} = 300 mV for this device.

It is quite apparent that a single defect is observable at the first two gate overdrives (Figs. 5a and 5b) and that this defect dominates in the sub-threshold regime. The highest gate overdrive (Fig. 5c) clearly shows the second low-frequency RTN defect which has a much less dominating effect. For the purpose of clarity we refer to the large high-frequency RTN fluctuation as defect #1 and smaller low frequency RTN fluctuation as defect #2.

To further explore these two distinct RTN signatures, we extract $\tau_{capture}$ and $\tau_{emission}$ for each of the defects as a function of gate overdrive (Fig. 6). At-low gate overdrives only one RTN signature is observed; thus, time constant extraction is as described in the experimental section of this manuscript. At higher gate overdrives, the time series RTN data were subject to an additional smoothing filter to eliminate the higher frequency (defect #1) fluctuations. This allows for accurate time constant extraction for both the higher frequency (defect

Authorized licensed use limited to: NIST Research Library. Downloaded on September 30, 2009 at 15:40 from IEEE Xplore. Restrictions apply.

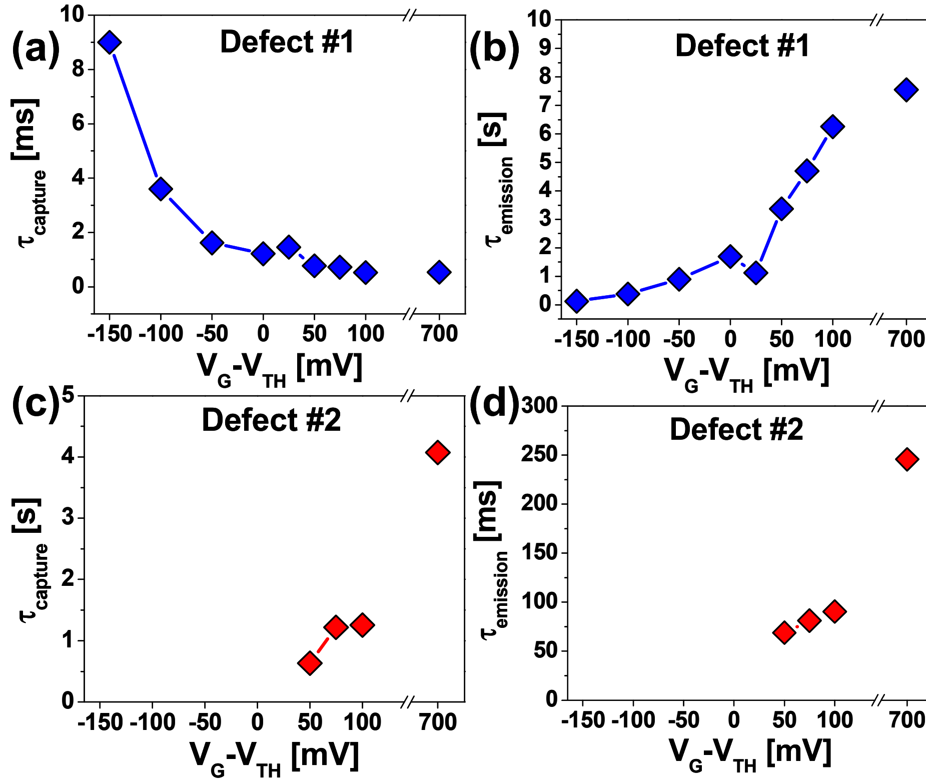

Figure 6. Extracted capture and emission time constants as a function of gate overdrive for defect 1 (a and b) as well as defect 2 (c and d), respectively. We note that extracted values are much larger than expected for this device structure (t_{ox} = 1.4 nm). V_{TH} = 300 mV for this device.

#1) and lower frequency (defect #2) defects as a function of gate overdrive. We observe gate overdrive dependent $\tau_{capture}$ and $\tau_{emission}$ values that range from approximately 1 ms to 10 s. It is important to note that our extracted time constant values are quite consistent with those reported in the literature for a large range of dielectric thicknesses [2]. While many researchers would use these extracted time constants to infer information about the trapping kinetics or capture cross sections associated with the aforementioned defects, we instead choose to examine a much more fundamental noise issue. If the observed RTN is due to an elastic tunneling phenomenon, why are these time constants so large?

IV. Discussion

As mentioned above, the McWhorter model attributes 1/f noise to a distribution of time constants, each of which corresponds to a different elastic tunneling depth. Until recently, this model was difficult to directly test as the gate dielectrics were relatively thick and the corresponding elastic tunneling times were comparable to many of the experimentally reported time constants. However, in our experiment, the gate dielectric is quite thin (1.4 nm physical). This sets a clear tunneling time restriction which allows us to unambiguously examine the validity of the elastic tunneling picture. One can estimate the expected tunneling time from the tunneling front model [28-31]. This model yields the time required for a "tunneling front" to reach a given dielectric depth with an assumption of the time zero tunneling depth (τ_0). For this manuscript, we employ a slightly modified tunneling front model which accounts for the barrier modification due to an applied electric field [30]. In this model the tunneling distance ($z(t)$) is given by:

$$z(t)=\left(\frac{1}{qE_{ox}}\right)\left((\phi_B-E_{elec})-\left(\frac{3\hbar qE_{ox}}{4\sqrt{2m_{ox}}}\ln\left(\frac{t}{\tau_0}\right)+(\phi_B-E_{elec})^{3/2}\right)^{2/3}\right) \quad (1)$$

where E_{ox} is the applied dielectric field, ϕ_B is the Si/dielectric barrier height, E_{elec} is the energy level of the electron above the Si conduction band edge, m_{ox} is the effective mass of the electron in the dielectric, q is the electronic charge, and t is the tunneling front time. Fig. 7 illustrates these tunneling front calculations for two different nitrogen concentrations. As we are somewhat unsure of the exact nitrogen concentration in our SiON dielectrics, we believe these simulated nitrogen concentrations represent the relevant "worst-case" extremes. In our calculations, the addition of nitrogen is presumed to modify the SiO_2 barrier height and effective mass as proposed in [32]. We also account for the barrier height modification due to the quantization of the Si conduction band inversion layer electrons [33, 34].

An initial examination of Fig. 7 suggests that it will be quite difficult to resolve the discrepancies between the experimentally observed 1 ms to 10 s time constants with the

Authorized licensed use limited to: NIST Research Library. Downloaded on September 30, 2009 at 15:40 from IEEE Xplore. Restrictions apply.

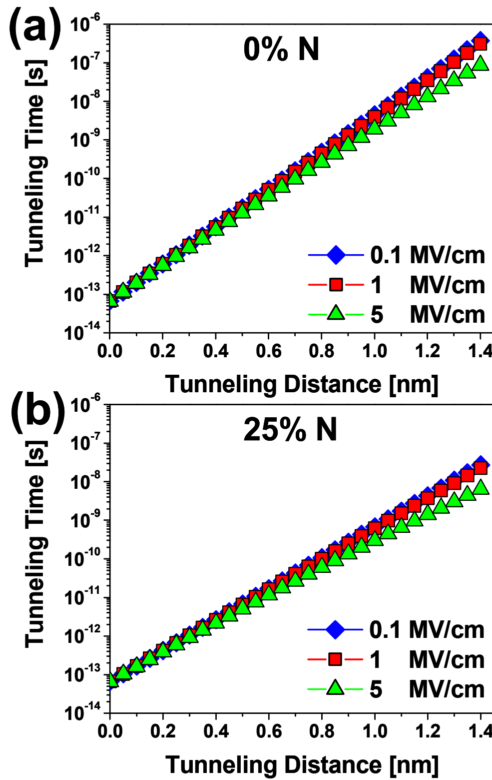

Figure 7. Tunneling front calculations for various dielectric fields and for pure SiO_2 (a) and 25 %N SiON (b). For these calculations $m_{ox}(SiO_2) = 0.4m_0$, $\phi_B = 3.1$ eV, $\tau_0 = 6.6 \times 10^{-14}$ s, and E_{elec} is assumed to correspond to the field-dependent 1st quantized energy state [33, 34]. The nitrogen modifications to m_{ox} and ϕ_B are given in [32].

much faster tunneling times. In the McWhorter picture, one would expect a maximum $\tau_{capture}$ when the defect is physically located at the poly-Si gate/dielectric interface. We note that this scenario is unphysical, as a defect in this position would dictate an emission time much faster than we could observe. The fast emission would make it seem as though there was no RTN in the time series (the offending defect would not be filled long enough to be measured). Regardless of this unphysical picture, we can use this situation as a "worst-case" scenario to test the elastic tunneling model. A defect located at the poly-Si gate/dielectric interface corresponds to a tunneling distance of 1.4 nm for our device structures. According to the tunneling front calculation, the maximum tunneling time for this distance is ≈3 x 10^{-7} s. Note that this time is at least 3 orders of magnitude faster than the fastest experimentally observed $\tau_{capture}$ (≈0.5 ms). We can also use the tunneling front calculation to examine the maximum $\tau_{emission}$ expected in the elastic tunneling picture. One would expect the maximum emission time when the defect is physically located near the middle of the dielectric. (If the defect is located closer to the top or bottom interface, the emission time diminishes.) In this "worst-case" $\tau_{emission}$ scenario, the corresponding tunneling distance (for the electron to tunnel out) would be approximately 0.7 nm. The maximum tunneling time for this defect distance (0.7 nm) is ≈150 ps. Note that this time is at least 8 orders of magnitude faster than the fastest experimentally observed $\tau_{emission}$ (≈60 ms). Thus, in both capture and emission, the elastic tunneling model predicts time constants which are several orders of magnitude faster than those experimentally observed.

We note that in this calculation, we use $\tau_0 = 6.6 \times 10^{-14}$ s [35]. Many other researchers use $\tau_0 = 10^{-10}$ s [18] for their calculations. This larger τ_0 value is actually based on speculation [36] while the 6.6 x 10^{-14} s was measured experimentally and supported by theoretical calculation [35]. Even if we were to use this larger τ_0 value in our tunneling front calculation, we would expect the calculated $\tau_{capture}$ and $\tau_{emission}$ times to increase approximately 3 orders of magnitude. While this course of action would allow for comparable experimental and theoretical $\tau_{capture}$ times, the experimental and theoretical $\tau_{emission}$ times would still disagree by 5 orders of magnitude. *This vast disagreement between the "worst-case" unphysical scenarios and our experimentally observed slower time constants compels us to conclude that the commonly accepted McWhorter elastic tunneling model for RTN and 1/f noise (and the subsequent analysis) must be incorrect.*

The realization that the elastic tunneling model is incorrect has left us to search for a more complete model which can explain the universally observed longer time constants (milliseconds to seconds). As mentioned above, several researchers have proposed other noise frameworks that include both inelastic tunneling of inversion layer charge to dielectric defects as well as interface state capture and emission [22, 23]. While these models are significantly more promising, they are not without some inadequacies. The inelastic tunneling model can easily explain the experimentally observed long $\tau_{emission}$ times. Unfortunately, it is not straight forward to understand how it can explain the experimentally observed longer $\tau_{capture}$ times (capture is still presumed to involve an initial elastic tunneling step). While it is possible that capture could be slowed by a phonon-assisted capture at higher energies, this is only speculation. Other researchers have invoked a noise framework involving capture and emission of inversion layer charge at interface state defects [24, 25]. While a cursory Shockley-Read-Hall calculation [37, 38] would suggest that capture and emission must occur at very deep interface states to be consistent with the longer time constants, there are major issues with this approach. Charge-pumping phenomena routinely operate at 1 MHz, implying an interface capture time (electron or hole by an interface state) of less than 0.5 µs. Thus, the expected interface state capture time is also many orders of magnitude faster than our observations. While we are unaware of a noise framework which is completely consistent with our observations, we find it likely that RTN is also occurring at higher frequencies (faster than our measurement equipment). Our simple calculations indicate that the tunneling barrier in our devices should be conducive to tunneling fluctuations in the 10^{-7} s to 10^{-10} s range (Fig. 7). Considering the possibility of these fast fluctuations, it is conceivable that our measurement bandwidth is limiting our (and all other researchers') observations to an incomplete picture. This bandwidth limitation may incorrectly preclude several existing noise theories.

Authorized licensed use limited to: NIST Research Library. Downloaded on September 30, 2009 at 15:40 from IEEE Xplore. Restrictions apply.

V. CONCLUSIONS

In this study, we have examined the origin of RTN fluctuations by extracting the characteristic capture and emission time constants ($\tau_{capture}$ and $\tau_{emission}$) as a function of gate overdrive. We note that our observed time constants and respective gate overdrive trends are not dissimilar to those reported in the literature. The distinguishing feature of our work is that we observe these time constants and trends at room temperature and in devices in which the dielectric cannot present a significant tunneling time contribution. Thus, a comparison of our extracted $\tau_{capture}$ and $\tau_{emission}$ values and those expected from the McWhorter model yields very large discrepancies. These observations strongly call into question much of the very recent literature that uses 1/f noise and RTN analysis to infer information about dielectric defects' energetic and spatial profiles. It is quite likely that these analyses (and the associated conclusions about bulk dielectric defect generation) need reinterpretation.

VI. ACKNOWLEDGMENTS

The authors would like to acknowledge fruitful conversations with C.A. Richter and T. Grasser. The authors acknowledge funding from the NIST Office of Microelectronics Programs. J.P.C. also acknowledges funding support by the National Research Council.

VII. REFERENCES

[1] G. Ghibaudo and T. Boutchacha, "Electrical Noise and RTS Fluctuations in Advanced CMOS Devices" *Microelectron. Reliab.,* **42**, pp. 573-582 (2002)

[2] M. J. Kirton and M. J. Uren, "Noise in Solid-State Microstructures - A New Perspective on Individual Defects, Interface States and Low-Frequency (1/f) Noise" *Adv. Phys.,* **38**, pp. 367-468 (1989)

[3] A. L. McWhorter, "1/f Noise and Germanium Surface Properties" in *Semiconductor Surface Physics*, R. H. Kingston, Ed. Philadelphia, PA: University of Pennsylvania Press, 1957, pp. 207-228.

[4] M. H. Tsai and T. P. Ma, "The Impact of Device Scaling on the Current Fluctuations in Mosfets" *IEEE Trans. Electron Dev.,* **41**, pp. 2061-2068 (1994)

[5] M. H. Tsai, T. P. Ma, and T. B. Hook, "Channel-Length Dependence of Random Telegraph Signal in Submicron MOSFETs" *IEEE Electron Device Lett.,* **15**, pp. 504-506 (1994)

[6] A. Ghetti, C. M. Compagnoni, F. Biancardi, A. L. Lacaita, S. Beltrami, L. Chiavarone, A. S. Spinelli, and A. Visconti, "Scaling Trends for Random Telegraph Noise in Deca-nanometer Flash Memories" *IEEE Int. Electron Dev. Meeting* pp. 835-838 (2008)

[7] H. Kurata, K. Otsuga, A. Kotabe, S. Kajiyama, T. Osabe, Y. Sasago, S. Narumi, K. Tokami, S. Kamohara, and O. Tsuchiya, "Random Telegraph Signal in Flash Memory: Its Impact on Scaling of Multilevel Flash Memory Beyond the 90-nm Node" *IEEE J. Solid-St. Circ.,* **42**, pp. 1362-1369 (2007)

[8] A. S. Spinelli, C. M. Compagnoni, R. Gusmeroli, M. Ghidotti, and A. Visconti, "Investigation of the Random Telegraph Noise Instability in Scaled Flash Memory Arrays" *Jpn. J. Appl. Phys.,* **47**, pp. 2598-2601 (2008)

[9] N. Tega, H. Miki, M. Yamaoka, H. Kume, M. Toshiyuki, T. Ishida, M. Yuki, R. Yamada, and T. Kazuyoshi, "Impact of Threshold Voltage Fluctuation Due to Random Telegraph Noise on Scaled-Down SRAM" *IEEE Int. Rel. Phys. Symp.* pp. 541-546 (2008)

[10] B. G. Min, S. P. Devireddy, Z. Celik-Butler, F. Wang, A. Zlotnicka, H. H. Tseng, and P. J. Tobin, "Low-frequency noise in submicrometer MOSFETs with HfO_2, HfO_2/Al_2O_3 and $HfAlO_x$ gate stacks" *IEEE Trans. Electron Dev.,* **51**, pp. 1679-1687 (2004)

[11] H. D. Xiong, H. Dawei, Y. Shuo, Z. Xiaoxiao, M. Gurfinkel, G. Bersuker, D. E. Ioannou, C. A. Richter, K. P. Cheung, and J. S. Suehle, "Stress-Induced Defect Generation in HfO_2/SiO_2 Stacks Observed by Using Charge Pumping and Low Frequency Noise Measurements" *IEEE Int. Rel. Phys. Symp.* pp. 319-323 (2008)

[12] H. D. Xiong, D. Heh, M. Gurfinkel, Q. Li, Y. Shapira, C. Richter, G. Bersuker, R. Choi, and J. S. Suehle, "Characterization of Electrically Active Defects in High-k Gate Dielectrics by Using Low Frequency Noise and Charge Pumping Measurements" *Microelectron. Eng.,* **84**, pp. 2230-2234 (2007)

[13] T. Grasser, B. Kaczer, T. Aichinger, W. Goes, and M. Nelhiebel, "Defect Creation Stimulated by Thermally Activated Hole Trappings as the Driving Force Behind Negative Bias Temperature Instability in SiO_2, SiON, and High-k Gate Stacks" *IEEE Int. Integrated Rel. Workshop Final Report,* pp. 91-95 (2008)

[14] K. S. Ralls, W. J. Skocpol, L. D. Jackel, R. E. Howard, L. A. Fetter, R. W. Epworth, and D. M. Tennant, "Discrete Resistance Switching in Submicrometer Silicon Inversion-Layers - Individual Interface Traps and Low-Frequency (1-F Questionable) Noise" *Phys. Rev. Lett.,* **52**, pp. 228-231 (1984)

[15] Z. Celik-Butler, P. Vasina, and N. Vibhavie Amarasinghe, "A Method for Locating the Position of Oxide Traps Responsible for Random Telegraph Signals in Submicron MOSFETs" *IEEE Trans. on Electron Dev.,* **47**, pp. 646-648 (2000)

[16] G. Ghibaudo, O. Roux, C. Nguyenduc, F. Balestra, and J. Brini, "Improved Analysis of Low-Frequency Noise in Field-Effect MOS-Transistors" *Phys. Status Solidi A,* **124**, pp. 571-581 (1991)

[17] K. K. Hung, P. K. Ko, C. M. Hu, and Y. C. Cheng, "A Unified Model for the Flicker Noise in Metal Oxide-Semiconductor Field-Effect Transistors" *IEEE Trans. Electron Dev.,* **37**, pp. 654-665 (1990)

[18] R. Jayaraman and C. G. Sodini, "A 1/F Noise Technique to Extract the Oxide Trap Density Near the Conduction-Band Edge of Silicon" *IEEE Trans. Electron Dev.,* **36**, pp. 1773-1782 (1989)

[19] N. Sghaier, L. Militaru, M. Trabelsi, N. Yacoubi, and A. Souifi, "Analysis of Slow Traps Centres in Submicron MOSFETs by Random Telegraph Signal Technique" *J. Microelectron,* **38**, pp. 610-614 (2007)

[20] Z. M. Shi, J. P. Mieville, and M. Dutoit, "Random Telegraph Signals in Deep-Submicron N-Mosfets" *IEEE Trans. Electron Dev.,* **41**, pp. 1161-1168 (1994)

[21] F. Wang and Z. Celik-Butler, "An Improved Physics-Based 1/f Noise Model for Deep Submicron MOSFETs" *Solid-State Electron.,* **45**, pp. 351-357 (2001)

[22] P. Dutta and P. M. Horn, "Low-Frequency Fluctuations in Solids - 1-F Noise" *Rev. Mod. Phys.,* **53**, pp. 497-516 (1981)

[23] M. B. Weissman, "1/F Noise and Other Slow, Nonexponential Kinetics in Condensed Matter" *Rev. Mod. Phys.,* **60**, pp. 537-571 (1988)

[24] H. E. Maes, S. H. Usmani, and G. Groeseneken, "Correlation Between 1/F Noise and Interface State Density at the Fermi Level in Field-Effect Transistors" *J. Appl. Phys.,* **57**, pp. 4811-4813 (1985)

[25] A. Ohata, A. Toriumi, M. Iwase, and K. Natori, "Observation of Random Telegraph Signals - Anomalous Nature of Defects at the Si/SiO_2 Interface" *J. Appl. Phys.,* **68**, pp. 200-204 (1990)

[26] J. P. Campbell, J. Qin, K. P. Cheung, L. Yu, J. S. Suehle, A. Oates, and K. Sheng, "The Origins of Random Telegraph Noise in Highly Scaled SiON nMOSFETs" *IEEE Int. Integrated Rel. Workshop Final Report,* pp. 105-109 (2008)

[27] S. Machlup, "Noise in Semiconductors - Spectrum of a 2-Parameter Random Signal" *J. Appl. Phys.,* **25**, pp. 341-343 (1954)

[28] F. P. Heiman and G. Warfield, "Effects of Oxide Traps on MOS Capacitance" *IEEE Trans. Electron Dev.,* **Ed12**, pp. 167-178 (1965)

[29] T. R. Oldham, A. J. Lelis, and F. B. Mclean, "Spatial Dependence of Trapped Holes Determined from Tunneling Analysis and Measured Annealing" *IEEE Trans. Nucl. Sci.,* **33**, pp. 1203-1209 (1986)

[30] Y. Wang, "High Frequency Techniques for Advanced MOS Device Characterization" *Ph. D. Thesis, Rutgers University, 2008*

[31] Y. Wang, V. Lee, and K. P. Cheung, "Frequency Dependent Charge-Pumping, How Deep Does It Probe?" *IEEE Int. Electron Dev. Meeting,* pp. 763-766 (2006)

[32] P. A. Kraus, K. Z. Ahmed, C. S. Olsen, and F. Nouri, "Model to Predict Gate Tunneling Current of Plasma Oxynitrides" *IEEE Trans. Electron Dev.,* **52**, pp. 1141-1147 (2005)

[33] S. A. Hareland, S. Krishnamurthy, S. Jallepalli, C. F. Yeap, K. Hasnat, A. F. Tasch, and C. M. Maziar, "A Computationally Efficient Model for

Authorized licensed use limited to: NIST Research Library. Downloaded on September 30, 2009 at 15:40 from IEEE Xplore. Restrictions apply.

Inversion Layer Quantization Effects in Deep Submicron N-channel MOSFET's" *IEEE Trans. Electron Dev.,* **43**, pp. 90-96 (1996)
[34] F. Stern, "Self-Consistent Results for N-Type Si Inversion Layers" *Phys. Rev. B,* **5**, pp. 4891-4899 (1972)
[35] I. Lundstrom and C. Svensson, "Tunneling to Traps in Insulators" *J. Appl. Phys.,* **43**, pp. 5045-5047 (1972)
[36] S. Christensson, I. Lundstrom, and C. Svensson, "Low Frequency Noise in MOS Transistors I: Theory" *Solid State Electron,* **11**, p. 797 (1968)
[37] R. N. Hall, "Electron-Hole Recombination in Germanium" *Phys. Rev.,* **87**, pp. 387-387 (1952)
[38] W. Shockley and W. T. Read, "Statistics of the Recombination of Holes and Electrons" *Phys. Rev.,* **87**, pp. 835-842 (1952)

Authorized licensed use limited to: NIST Research Library. Downloaded on September 30, 2009 at 15:40 from IEEE Xplore. Restrictions apply.